INTERNATIONAL STANDARD

ISO 25178-604

First edition
2013-08-01

Geometrical product specifications (GPS) — Surface texture: Areal —

Part 604: Nominal characteristics of non-contact (coherence scanning interferometry) instruments

Spécification géométrique des produits (GPS) — État de surface: Surfacique —

Partie 604: Caractéristiques nominales des instruments sans contact (à interférométrie par balayage à cohérence)

Reference number
ISO 25178-604:2013(E)

COPYRIGHT PROTECTED DOCUMENT

ISO copyright office
Case postale 56 • CH-1211 Geneva 20
Tel. + 41 22 749 01 11
Fax + 41 22 749 09 47
E-mail copyright@iso.org
Web www.iso.org

Published in Switzerland

Contents

Page

Foreword

ISO (the International Organization for Standardization) is a worldwide federation of national standards bodies (ISO member bodies). The work of preparing International Standards is normally carried out through ISO technical committees. Each member body interested in a subject for which a technical committee has been established has the right to be represented on that committee. International organizations, governmental and non-governmental, in liaison with ISO, also take part in the work. ISO collaborates closely with the International Electrotechnical Commission (IEC) on all matters of electrotechnical standardization.

The procedures used to develop this document and those intended for its further maintenance are described in the ISO/IEC Directives, Part 1. In particular the different approval criteria needed for the different types of ISO documents should be noted. This document was drafted in accordance with the editorial rules of the ISO/IEC Directives, Part 2. www.iso.org/directives

Attention is drawn to the possibility that some of the elements of this document may be the subject of patent rights. ISO shall not be held responsible for identifying any or all such patent rights. Details of any patent rights identified during the development of the document will be in the Introduction and/or on the ISO list of patent declarations received. www.iso.org/patents

Any trade name used in this document is information given for the convenience of users and does not constitute an endorsement.

The committee responsible for this document is ISO/TC 213, *Dimensional and geometrical product specifications and verification.* The document was prepared in collaboration with Technical Committee CEN/TC 290, *Dimensional and geometrical product specifications and verification*.

ISO 25178 consists of the following parts, under the general title *Geometrical product specifications (GPS) — Surface texture: Areal*:

— Part 1: *Indication of surface texture*

— *Part 2: Terms, definitions and surface texture parameters*

— *Part 3: Specification operators*

— *Part 6: Classification of methods for measuring surface texture*

— *Part 70: Physical measurement standards*

— *Part 71: Software measurement standards*

— *Part 601: Nominal characteristics of contact (stylus) instruments*

— *Part 602: Nominal characteristics of non-contact (confocal chromatic probe) instruments*

— *Part 603: Nominal characteristics of non-contact (phase shifting interferometric microscopy) instruments*

— *Part 604: Nominal characteristics of non-contact (coherence scanning interferometry) instruments*

— *Part 605: Nominal characteristics of non-contact (point autofocus probe) instruments*

— *Part 606: Nominal characteristics of non-contact (focus variation) instruments*

— *Part 701: Calibration and measurement standards for contact (stylus) instruments*

The following part is under preparation:

— *Part 72: XML file format x3p*

Introduction

This part of ISO 25178 is a geometrical product specification (GPS) standard and is to be regarded as a general GPS standard (see ISO/TR 14638). It influences chain link 5 of the chains of standards on roughness profile, waviness profile, primary profile and areal surface texture.

The ISO/GPS Masterplan given in ISO/TR 14638 gives an overview of the ISO/GPS system of which this document is a part. The fundamental rules of ISO/GPS given in ISO 8015 apply to this document and the default decision rules given in ISO 14253-1 apply to specifications made in accordance with this document, unless otherwise indicated.

For more detailed information on the relation of this part of ISO 25178 to other standards and to the GPS matrix model, see Annex E.

This part of ISO 25178 describes the metrological characteristics of coherence scanning interferometric microscopes, designed for the measurement of surface topography maps. For more detailed information on the coherence scanning technique, see Annex A and Annex B.

NOTE Portions of this document, particularly the informative texts, may describe patented systems and methods. This information is provided only to assist users in understanding the operating principles of coherence scanning interferometry. This document is not intended to establish priority for any intellectual property, nor does it imply a license to any proprietary technologies that may be described herein.

Geometrical product specifications (GPS) — Surface texture: Areal —

Part 604: Nominal characteristics of non-contact (coherence scanning interferometry) instruments

1 Scope

This part of ISO 25178 specifies the metrological characteristics of coherence scanning interferometry (CSI) systems for 3D mapping of surface height.

2 Terms and definitions

For the purposes of this document, the following terms and definitions apply.

2.1 Terms and definitions related to all areal surface texture measurement methods

2.1.1
areal reference
component of the instrument that generates a reference surface with respect to which the surface topography is measured

2.1.2
coordinate system of the instrument
right hand orthonormal system of axes (x, y, z) defined as:

— (x, y) is the plane established by the areal reference of the instrument (note that there are optical instruments that do not possess a physical areal guide)

— z-axis is mounted parallel to the optical axis and is perpendicular to the (x, y) plane for an optical instrument; the z-axis is in the plane of the stylus trajectory and is perpendicular to the (x, y) plane for a stylus instrument (see Figure 1)

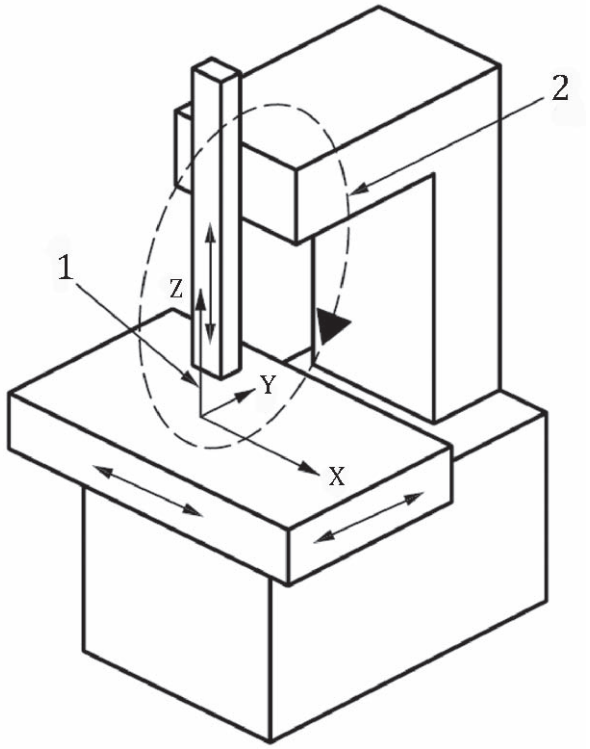

Key

1 coordinate system of the instrument

2 measurement loop

Figure 1 — Coordinate system and measurement loop of the instrument

Note 1 to entry: Normally, the *x*-axis is the tracing axis and the *y*-axis is the stepping axis. (This note is valid for instruments that scan in the horizontal plane.)

Note 2 to entry: See also "specification coordinate system" [ISO 25178-2:2012, 3.1.2] and "measurement coordinate system" [ISO 25178-6:2010, 3.1.1].

2.1.3
measurement loop

closed chain which comprises all components connecting the workpiece and the probe, e.g. the means of positioning, the work holding fixture, the measuring stand, the drive unit, the probing system

Note 1 to entry: The measurement loop will be subjected to external and internal disturbances that influence the measurement uncertainty.

SEE: Figure 1.

2.1.4
real surface of a workpiece

set of features which physically exist and separate the entire workpiece from the surrounding medium

Note 1 to entry: The real surface is a mathematical representation of the surface that is independent of the measurement process.

Note 2 to entry: See also "mechanical surface" [ISO 25178-2:2012, 3.1.1.1 or ISO 14406:2010, 3.1.1] and "electromagnetic surface" [ISO 25178-2:2012, 3.1.1.2 or ISO 14406:2010, 3.1.2].

Note 3 to entry: The electro-magnetic surface considered for one type of optical instrument may be different from the electro-magnetic surface for other types of optical instruments.

2.1.5
surface probe
device that converts the surface height into a signal during measurement

Note 1 to entry: In earlier standards, this was termed “transducer”.

2.1.6
measuring volume
range of the instrument stated in terms of the limits on all three coordinates measured by the instrument

Note 1 to entry: For areal surface texture measuring instruments, the measuring volume is defined by the measuring range of the *x*- and *y*- drive units, and the measuring range of the *z*-probing system.

[SOURCE: ISO 25178-601:2010, 3.4.1]

2.1.7
response curve
F_x, F_y, F_z
graphical representation of the function that describes the relation between the actual quantity and the measured quantity

Note 1 to entry: An actual quantity in x (respectively y or z) corresponds to a measured quantity x_M (respectively y_M or z_M).

Note 2 to entry: The response curve can be used for adjustments and error corrections.

[SOURCE: ISO 25178-601:2010, 3.4.2]

2.1.8
amplification coefficient
α_x, α_y, α_z
slope of the linear regression curve obtained from the r*esponse curve* (2.1.7)

Note 1 to entry: There will be amplification coefficients applicable to the *x*, *y* and *z* quantities.

Note 2 to entry: The ideal response is a straight line with a slope equal to 1, which means that the values of the measurand are equal to the values of the input quantities.

Note 3 to entry: See also “sensitivity of a measuring system” (ISO/IEC Guide 99:2007,[1] 4.12)

[SOURCE: ISO 25178-601:2010, 3.4.3, modified —Note 3 to entry has been added.]

2.1.9
instrument noise
N_i
internal noise added to the output signal caused by the instrument if ideally placed in a noise-free environment

Note 1 to entry: Internal noise can be due to electronic noise, as e.g. amplifiers, or optical noise, as e.g. stray light.

Note 2 to entry: This noise typically has high frequencies and it limits the ability of the instrument to detect small spatial wavelengths of the surface texture.

Note 3 to entry: The S-filter according ISO 25178-3 may reduce this noise.

Note 4 to entry: For some instruments, instrument noise cannot be estimated because the instrument only takes data while moving.

2.1.10
measurement noise
N_M
noise added to the output signal occurring during the normal use of the instrument

Note 1 to entry: Notes 2 and 3 of 2.1.9 apply as well to this definition.

Note 2 to entry: Measurement noise includes *instrument noise* (2.1.9).

2.1.11
surface topography repeatability
repeatability of topography map in successive measurements of the same surface under the same conditions of measurement

Note 1 to entry: Surface topography repeatability provides a measure of the likely agreement between repeated measurements normally expressed as a standard deviation.

Note 2 to entry: See ISO/IEC Guide 99:2007,[1] 2.15 and 2.21, for a general discussion of repeatability and related concepts.

Note 3 to entry: Evaluation of surface topography repeatability is a common method for determining the measurement noise.

2.1.12
sampling interval in x
D_x
distance between two adjacent measured points along the x-axis

Note 1 to entry: In many microscopy systems, the sampling interval is determined by the distance between sensor elements in a camera, called pixels. For such systems, the terms pixel pitch and pixel spacing are often used interchangeably with the term sampling interval. Another term, pixel width, indicates a length associated with one side (x or y) of the sensitive area of a single pixel and is always smaller than the pixel spacing. Yet another term, sampling zone, may be used to indicate the length or region over which a height sample is determined. This quantity could either be larger or smaller than the sampling interval.

2.1.13
sampling interval in y
D_y
distance between two adjacent measured points along the y-axis

Note 1 to entry: In many microscopy systems, the sampling interval is determined by the distance between sensor elements in a camera, called pixels. For such systems, the terms pixel pitch and pixel spacing are often used interchangeably with the term sampling interval. Another term, pixel width, indicates a length associated with one side (x or y) of the sensitive area of a single pixel and is always smaller than the pixel spacing. Yet another term, sampling zone, may be used to indicate the length or region over which a height sample is determined. This quantity could either be larger or smaller than the sampling interval.

2.1.14
digitization step in z
D_z
smallest height variation along the z-axis between two ordinates of the extracted surface

2.1.15
lateral resolution
R_l
smallest distance between two features which can be detected

[SOURCE: ISO 25178-601:2010, 3.4.10, modified —The word “separation” has been removed before “distance”.]

2.1.16
width limit for full height transmission
W_l
width of the narrowest rectangular groove whose measured height remains unchanged by the measurement

Note 1 to entry: Instrument properties (such as the sampling interval in x and y, the digitization step in z, and the short wavelength cutoff filter) should be chosen so that they do not influence the lateral resolution and the width limit for full height transmission.

Note 2 to entry: When determining this parameter by measurement, the depth of the rectangular groove should be close to that of the surface to be measured.

[SOURCE: ISO 25178-601:2010, 3.4.11, modified —The notes have been changed.]

2.1.17
lateral period limit
D_{LIM}
spatial period of a sinusoidal profile at which the height response of an instrument falls to 50 %

Note 1 to entry: The lateral period limit is one metric for describing spatial or lateral resolution of a surface topography measuring instrument and its ability to distinguish and measure closely spaced surface features. Its value depends on the heights of surface features and on the method used to probe the surface. Maximum values for this parameter are listed in ISO 25178-3:2012, Table 3, in comparison with recommended values for short wavelength (s-)filters and sampling intervals.

Note 2 to entry: Spatial period is the same concept as *spatial wavelength* and is the inverse of *spatial frequency*.

Note 3 to entry: One factor related to the value of D_{LIM} for optical tools is the *Rayleigh criterion* (2.3.7). Another is the degree of focus of the objective on the surface.

Note 4 to entry: One factor related to the value of D_{LIM} for contact tools is the stylus tip radius, r_{TIP} (see ISO 25178-601).

Note 5 to entry: Other terms related to *lateral period limit* are *structural resolution* and *topographic spatial resolution.*

2.1.18
maximum local slope
greatest local slope of a surface feature that can be assessed by the probing system

Note 1 to entry: The term “local slope” is defined in ISO 4287:1997, 3.2.9.

2.1.19
instrument transfer function
ITF
f_{ITF}
function of spatial frequency describing how a surface topography measuring instrument responds to an object surface topography having a specific spatial frequency

Note 1 to entry: Ideally, the ITF tells us what the measured amplitude of a sinusoidal grating of a specified spatial frequency ν would be relative to the true amplitude of the grating.

Note 2 to entry: For several types of optical instruments, the ITF may be a nonlinear function of height except for heights much smaller than the optical wavelength.

2.1.20
hysteresis
x_{HYS}, y_{HYS}, z_{HYS}
property of measuring equipment, or characteristic whereby the indication of the equipment or value of the characteristic depends on the orientation of the preceding stimuli

Note 1 to entry: Hysteresis can also depend, for example, on the distance travelled after the orientation of stimuli has changed.

Note 2 to entry: For lateral scanning systems, the hysteresis is mainly a repositioning error.

[SOURCE: ISO 14978:2006, 3.24, modified —Note 2 to entry and the symbols have been added.]

2.1.21
metrological characteristic
metrological characteristic of a measuring instrument
<measuring equipment> characteristic of measuring equipment, which may influence the results of measurement

Note 1 to entry: Calibration of metrological characteristics may be necessary.

Note 2 to entry: The metrological characteristics have an immediate contribution to measurement uncertainty.

Note 3 to entry: Metrological characteristics for areal surface texture measuring instruments are given in Table 1.

Table 1 — List of metrological characteristics for surface texture measurement methods

Metrological characteristic	Symbol	Definition	Main potential error along
Amplification coefficient	α_x, α_y, α_z	2.1.8	x, y, z
Linearity deviation	l_x, l_y, l_z	Maximum local difference between the line from which the amplification coefficient is derived and the response curve.	x, y, z
Residual flatness	z_{FLT}	Flatness of the areal reference	z
Measurement noise	N_M	2.1.10	z
Lateral period limit	D_{LIM}	2.1.17.	z
Perpendicularity	Δ_{PERxy}	Deviation from 90° of the angle between the x- and y-axes	x, y

[SOURCE: ISO 14978:2006, 3.12, modified — The notes are different and the table has been added.]

2.2 Terms and definitions related to *x*- and *y*-scanning systems

2.2.1
areal reference guide
component(s) of the instrument that generate(s) the reference surface, in which the probing system moves relative to the surface being measured according to a theoretically exact trajectory

Note 1 to entry: In the case of *x*- and *y*-scanning areal surface texture measuring instruments, the areal reference guide establishes a reference surface [ISO 25178-2:2012, 3.1.8]. It can be achieved through the use of two linear and perpendicular reference guides [ISO 3274:1996, 3.3.2] or one reference surface guide.

2.2.2
lateral scanning system
system that performs the scanning of the surface to be measured in the (x, y) plane

Note 1 to entry: There are essentially four aspects to a surface texture scanning instrument system: the x-axis drive, the y-axis drive, the z-measurement probe and the surface to be measured. There are different ways in which these may be configured and thus there will be a difference between different configurations as explained in Table 2.

Note 2 to entry: When a measurement consists of a single field of view of a microscope, *x*- and *y*-scanning is not used. However, when several fields of view are linked together by stitching methods, see Reference [2] the system is considered to be a scanning system.

Table 2 — Possible different configurations for reference guides (*x* and *y*)

		Drive unit				
		Two reference guides (*x* and *y*)[a]			One areal reference guide	
		P*x* o C*y*	P*x* o P*y*	C*x* o C*y*	P*xy*	C*xy*
Probing System	A: without arcuate error correction	P*x* o C*y*-A	P*x* o P*y*-A	C*x* o C*y*-A	P*xy*-A	C*xy*-A
	S: without arcuate error or with arcuate error corrected	P*x* o C*y*-S	P*x* o P*y*-S	C*x* o C*y*-S	P*xy*-S	C*xy*-S

a For two given functions *f* and *g*, *f* o *g* is the combination of these functions

P*x* = probing systems moving along the *x*-axis

P*y* = probing systems moving along the *y*-axis

C*x* = component moving along the *x*-axis

C*y* = component moving along the *y*-axis

2.2.3
drive unit *x*
component of the instrument that moves the probing system or the surface being measured along the reference guide on the *x*-axis and returns the horizontal position of the measured point in terms of the lateral *x* coordinate of the profile

2.2.4
drive unit *y*
component of the instrument that moves the probing system or the surface being measured along the reference guide on the *y*-axis and returns the horizontal position of the measured point in terms of the lateral *y* coordinate of the profile

2.2.5
lateral position sensor
component of the drive unit that provides the lateral position of the measured point

Note 1 to entry: The lateral position can be measured or inferred by using, for example, a linear encoder, a laser interferometer, or a counting device coupled with a micrometre screw.

2.2.6
speed of measurement
v_x
speed of the probing system relative to the surface to be measured during the measurement along the *x*-axis

[SOURCE: ISO 25178-601:2010, 3.4.13]

2.2.7
static noise
N_S
combination of the *instrument noise* (2.1.9) and environmental noise on the output signal when the instrument is not scanning laterally

Note 1 to entry: Environmental noise is caused by e.g. seismic, sonic and external electromagnetic disturbances.

Note 2 to entry: Notes 2 and 3 in 2.1.9 also apply to this definition.

Note 3 to entry: Static noise is included in *measurement noise* (2.1.10)

2.2.8
dynamic noise
N_D
noise occurring during the motion of the drive units on the output signal

Note 1 to entry: Notes 2 and 3 in 2.1.9 also apply to this definition.

Note 2 to entry: Dynamic noise includes the static noise.

Note 3 to entry: Dynamic noise is included in *measurement noise* (2.1.10).

2.3 Terms and definitions related to optical systems

2.3.1
light source
optical device emitting an appropriate range of wavelengths in a specified spectral region

2.3.2
measurement optical bandwidth
$B_{\lambda 0}$
range of wavelengths of light used to measure a surface

Note 1 to entry: Instruments may be constructed with light sources with a limited optical bandwidth and/or with additional filter elements to further limit the optical bandwidth.

2.3.3
measurement optical wavelength
λ_0
effective value of the wavelength of the light used to measure a surface

Note 1 to entry: The measurement optical wavelength is affected by conditions such as the light source spectrum, spectral transmission of the optical components, and spectral response of the image sensor array.

2.3.4
angular aperture
angle of the cone of light entering an optical system from a point on the surface being measured

[SOURCE: ISO 25178-602:2010, 3.3.3]

2.3.5
half aperture angle
α
one half of the angular aperture

Note 1 to entry: This angle is sometimes called the “half cone angle” (see Figure 2).

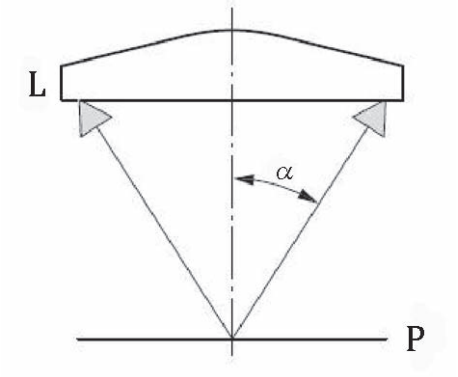

Key

L lens or optical system

P focal point

α half aperture angle

Figure 2 — Half aperture angle

2.3.6
numerical aperture
A_N
sine of the half aperture angle multiplied by the refractive index n of the surrounding medium

$$A_N = n \sin\alpha$$

Note 1 to entry: In air for visible light, $n \cong 1$.

Note 2 to entry: The numerical aperture is dependent on the wavelength of light. Typically, the numerical aperture is specified for the wavelength that is in the middle of the measurement optical bandwidth.

2.3.7
Rayleigh criterion
quantity characterizing the spatial resolution of an optical system given by the separation of two point sources at which the first diffraction minimum of the image of one point source coincides with the maximum of the other

Note 1 to entry: For a theoretically perfect, incoherent optical system with a filled objective pupil, the Rayleigh criterion of the optical system is equal to $0{,}61\ \lambda_0/A_N$.

Note 2 to entry: This parameter is useful for characterizing the instrument response to features with heights much less than λ_0 for optical 3D metrology instruments.

2.3.8
Sparrow criterion
quantity characterizing the spatial resolution of an optical system given by the separation of two point sources at which the second derivative of the intensity distribution vanishes between the two imaged points

Note 1 to entry: For a theoretically perfect, incoherent optical system with filled objective pupil, the Sparrow criterion of the optical system is equal to $0{,}47\ \lambda_0/A_N$, approximately 0,77 times the *Rayleigh criterion* (2.3.7).

Note 2 to entry: This parameter is useful for characterizing the instrument response to features with heights much less than λ_0 for optical 3D metrology instruments.

Note 3 to entry: Under the same measurement conditions as the notes above, the Sparrow criterion is nearly equal to the spatial period of $0{,}50\ \lambda_0/A_N$, for which the theoretical instrument response falls to zero.

2.4 Terms and definitions related to optical properties of the workpiece

2.4.1
surface film
material deposited onto another surface whose optical properties are different from that surface

Note 1 to entry: This concept may also be called “surface layer”.

2.4.2
thin film
film whose thickness is such that the top and bottom surfaces cannot be readily separated by the optical measuring system

Note 1 to entry: For some measurement systems with special properties and algorithms, the thicknesses of thin films may be derived.

2.4.3
thick film
film whose thickness is such that the top and bottom surfaces can be readily separated by the optical measuring system

2.4.4
optically smooth surface
surface from which the reflected light is primarily specular and scattered light is not significant

Note 1 to entry: An optically smooth surface behaves locally like a mirror.

Note 2 to entry: A surface that acts as optically smooth under certain conditions, such as wavelength range, numerical aperture, pixel resolution, etc. can act as optically rough when one or more of these conditions change.

2.4.5
optically rough surface
surface that does not behave as an optically smooth surface, i.e. where scattered light is significant

Note 1 to entry: A surface that acts as optically rough under certain conditions, such as wavelength range, numerical aperture, pixel resolution, etc. can act as optically smooth when one or more of these conditions change.

2.4.6
optically non-uniform material
sample with different optical properties in different regions

Note 1 to entry: An optically non-uniform material may result in measured phase differences across the field of view that can be erroneously interpreted as differences in surface height.

2.5 Terms and definitions specific to coherence scanning interferometric microscopy

2.5.1
coherence scanning interferometry
CSI
surface topography measurement method wherein the localization of interference fringes during a scan of optical path length provides a means to determine a surface topography map

Note 1 to entry: CSI encompasses but is not limited to instruments that use spectrally broadband, visible sources (white light) to achieve interference fringe localization.

Note 2 to entry: CSI uses either fringe localization alone or in combination with interference phase evaluation, depending on the surface type, desired surface topography repeatability and software capabilities.

Note 3 to entry: Table 3 compiles alternative terms that conform at least in part to the above definition.

Table 3 — Summary of recognized terms for CSI

Acronym	Term	Bibliography reference
CSI	Coherence scanning interferometry	[3]
CPM	Coherence probe microscope	[4]
CSM	Coherence scanning microscope	[5]
CR	Coherence radar	[6]
CCI	Coherence correlation interferometry	[7]
MCM	Mirau correlation microscope	[8]
WLI	White light interferometry	[9]
WLSI	White light scanning interferometry	[10]
SWLI	Scanning white light interferometry	[11]
WLPSI	White light phase shifting interferometry	[12]
VSI	Vertical scanning interferometry	[10]
EVSI	Enhanced VSI	[10]
HDVSI	High-definition Vertical Scanning Interferometry	[13]
RSP	Rough surface profiler	[14]
RST	Rough surface tester	[15]
HIS	Height scanning interferometer	[16]
IRS	Infrared scanning	[17]

[SOURCE: ISO 25178-6:2010, 3.3.5]

2.5.2
optical path length
physical distance a light beam travels multiplied by the index of refraction of the traversed medium

Note 1 to entry: The optical path difference in a two-beam interferometer is the difference in optical path length between the reference path and measurement path.

2.5.3
coherence scanning interferometry signal
CSI signal
intensity data recorded for an individual image point or camera pixel as a function of scan position

Note 1 to entry: See Figure 3 and A.1.

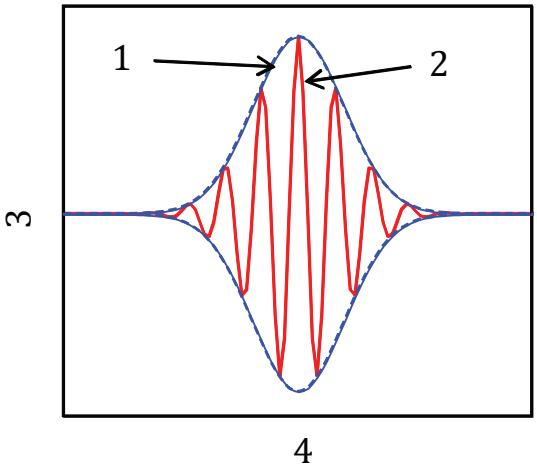

Key

1 modulation envelope (calculated)
2 CSI signal
3 intensity
4 scan position

Figure 3 — Typical CSI signal

2.5.4
interference fringes
rapidly modulating portion of the CSI signal, related to the interference effect and generated by the variation of optical path length during the CSI scan

Note 1 to entry: The interference fringes are approximately sinusoidal as a function of scan position.

Note 2 to entry: The distance between interference-fringe peaks corresponds to scan position differences that are approximately one-half the effective mean wavelength of the light source (see 2.3.1).

SEE: Figure 3.

2.5.5
interference phase
argument of the sine function used to approximate the form of interference fringes

Note 1 to entry: A complete fringe oscillation or period is equal to a 2π change in phase.

2.5.6
amplitude modulation
peak-to-valley or equivalent measure of the CSI signal

Note 1 to entry: Amplitude modulation depends mainly on radiance of the light source, camera sensitivity, and reflectivities of object and reference mirror.

Note 2 to entry: Amplitude modulation is also often termed “signal strength”.

SEE: Figure 3.

2.5.7
modulation envelope
overall variation in amplitude modulation of a CSI signal as a function of scan position

Note 1 to entry: The modulation envelope (Figure 3) is not necessarily a rigorously-defined aspect of the signal. The quantitative shape of the envelope is related closely to the means by which it is calculated.

Note 2 to entry: The modulation envelope is most closely associated with the idea of fringe localization, which is a basic characteristic of CSI signals.

Note 3 to entry: The modulation envelope is a consequence of limited optical coherence, which follows from using a spectrally-broadband light source (white light), a spatially extended light source, or both.

2.5.8
analysis mode
signal processing option
processing selection that determines whether the software makes use of the modulation envelope alone to measure surface heights or both the envelope and the interference fringe phase

2.5.9
modulation threshold
minimum modulation
D_{MOD}
lowest amplitude modulation deemed usable by the software for further evaluation of surface height

Note 1 to entry: The minimum modulation level typically provides a selection for valid data points. Those points with amplitude modulation falling below this level are considered invalid.

2.5.10
coherence scanning interferometry scan
CSI scan
mechanical or optical scan which varies the optical length of either the reference path or measurement path to generate a signal that exhibits interference fringes

Note 1 to entry: In CSI microscopes, the most common (but not exclusive) scanning means is a physical translation of an interference objective, which is pre-adjusted such that the peak CSI signal intensity coincides with the position of best focus.

2.5.11
scan length
z_{TOT}
total range of physical path length traversed by the CSI scan

Note 1 to entry: The scan length is usually synonymous with the total displacement of a moving component of the interferometer mechanically translated along its optical axis during data acquisition. The moving component could be, for example, an interference objective or a mirror in the reference arm or the complete interferometer moving with respect to the surface.

SEE: A.5.

2.5.12
scan increment
$\Delta_{\boldsymbol{z}}$
distance travelled by the CSI scan between individual images captured by the camera (camera frames) or individual data acquisition points

Note 1 to entry: The scan increment is commonly equivalent to 4 frames per interference fringe, but can be any number of frames.

2.5.13
scan speed
v_z
velocity of the CSI scan

Note 1 to entry: This can be expressed e.g. in micrometres per second.

2.5.14
effective mean wavelength
twice the period of the interference fringe closest to the modulation envelope peak

Note 1 to entry: The period of an interference fringe is the scan distance separating two neighbouring peaks in the CSI signal.

Note 2 to entry: The effective mean wavelength is a function of the *measurement optical wavelength* (2.3.3), the optical geometry and the data acquisition method, see Reference [18].

2.5.15
fringe-order error
error in the identification of the correct fringe when calculating relative heights using interference phase for surface topography calculations

Note 1 to entry: Fringe-order errors in CSI can be the result of errors in the analysis of the modulation envelope.

Note 2 to entry: Fringe-order errors are integer multiples of one-half the equivalent wavelength in height.

Note 3 to entry: Fringe-order errors are sometimes termed 2π errors.

2.5.16
environmental vibration
N_{VIB}
mechanical motions that disturb the CSI scan in an unpredictable and unwanted way, leading to measurement errors

Note 1 to entry: Environmental vibration may be caused by various sources (e.g. seismic, sonic and external electro-magnetic disturbances), see B.6.

3 Descriptions of the influence quantities

3.1 General

CSI instruments provide a measurement of lateral (x, y) and height (z) values from which surface shape and texture parameters are calculated.

3.2 Influence quantities

Influence quantities for CSI instruments are given in Table 4, which also indicates the metrological characteristics (see 2.1.21, Table 1) that are affected by deviations of the influence quantities.

NOTE For a theoretically perfect, incoherent optical system with a filled objective pupil and when measuring features with heights much smaller than λ_0, the lateral period limit D_{LIM} (2.1.17) of CSI systems is at least twice the *Rayleigh criterion* (2.3.7).

Table 4 — Influence quantities for coherence scanning interferometry

Component	Element	Influence quantities		Metrological characteristic affected ...
Light source		λ_0	Measurement optical wavelength (See 2.3.3.)	α_z
		$B_{\lambda 0}$	Measurement optical bandwidth (See 2.3.2.)	α_z
		S, P, C, E, U	The state of polarization of the light impinging on the measured surface. The polarization is typically described as S, P, circular (C), elliptical (E), or unpolarized (U).	α_x, α_y, α_z
Interferometer imaging system		A_N	Microscope numerical aperture (2.3.6)	α_x, α_y, α_z, D_{LIM}
		M_{IMG}	Magnification between object sizes on the surface and image sizes on the sensor	α_x, α_y
		Δ_{PATH}	Wavefront distortion, a function describing net deviations in the measured optical path of the system, derived from deviations in both the reference and measurement arms	α_z
		Q_{OPT}	General quality of the optical components used, including aberrations, transmission, alignment errors, etc.	α_x, α_y, α_z, z_{FLT}, l_x, l_y, l_z, D_{LIM}, Δ_{PERxy}
		P_{DISxy}	Lateral distortion of the magnified image on the camera	α_x, α_y, z_{FLT}, l_x, l_y, D_{LIM}, Δ_{PERxy}
		$U_I(x, y)$	Illumination uniformity – Distribution of illumination across the field of view of the object (a highly uniform, constant distribution is desired)	α_x, α_y, α_z, z_{FLT}, l_x, l_y, l_z
Camera		Δ_x	x-pixel spacing of the imaging camera	D_{LIM}
		Δ_y	y-pixel spacing of the imaging camera	D_{LIM}
Controller	Acquisition Software	V_z	Scan speed (See 2.5.13, A.5 and B.4.)	α_z, l_z
		z_{TOT}	Scan length (See 2.5.11, A.5 and B.4.)	α_z, l_z
		Δ_z	Scan Increment (See 2.5.12, A.5 and B.4.)	α_z
		$\Delta_{z\text{-LIN}}$	Scan linearity (See A.5 and B.4.)	α_z, l_z
		T_I	Integration time required to complete a single scan in z	N_M
		D_z	Height digitization step	N_M
	Profile Analysis Software	A_{ALG}	Measurement algorithm – Method for interpreting the CSI signal, including the option of using phase information (See B.3.)	α_z, l_z
		D_{MOD}	Fringe intensity modulation threshold - the minimum peak-valley intensity variation that the controller recognizes to be an interference fringe	α_z, l_z
		C_z	z-Cal factor, height adjustment coefficient	α_z, l_z
Instrument Overall		D_x or D_y	Lateral sampling interval, equal to the lateral pixel spacing of the camera (Δ_x, Δ_y) divided by the magnification	D_{LIM}
		N_I	Instrument noise (2.1.9)	N_M
		N_{VIB}	Environmental vibration (See B.6.)	N_M
		x_{HYS}, y_{HYS}, z_{HYS}	Hysteresis (2.1.19)	l_x, l_y, l_z

Table 4 *(continued)*

Component	Element	Influence quantities		Metrological characteristic affected ...
Sample		θ_{TLT}*	Tilt – Relative angle between the optical axis of the system and the sample normal. Object surface slopes that cause light to reflect at or near to the edge or outside of the numerical aperture of the objective A_N are also likely to cause significant signal loss.	α_x, α_y, α_z
		Φ_{DIS}*	The relative phase shift upon reflection of dissimilar materials.	α_z
		T_{FLM}*	Thickness of transparent or semi-transparent films. These films typically have thickness comparable to the illumination wavelength. Note that thinner contamination or native oxide films do not necessarily affect the CSI measurement process.	α_z
		T_{MED}*	Thick transparent media - transparent media (such as cover glass or liquid) between the sample and the instrument.	α_z
		URF*	Under resolved features - Object features having dimensions on the order of or smaller than the lateral resolution. (See Annex C.)	α_z
		*NOTE These influence quantities arise from the interaction between the instrument and the sample being measured.		

Annex A
(informative)

Overview and components of a coherence scanning interferometry (CSI) microscope

A.1 Overview

CSI instruments use the following measurement process.

— The instrument is focused on the surface as indicated by the appearance of interference fringes.

— For measurement of randomly rough surfaces, the sample tilt relative to the optical axis of the system is adjusted to minimize the number of fringes across the field of view. For measurement of step features on smooth surfaces, a sample tilt adjusted to provide one or more fringes across the field of view and perpendicular to the step may be useful.

— The instrument executes a data acquisition during a CSI scan.

— Data analysis using either the modulation envelope, the interference fringes, or both, results in a surface topography map.

Deviations of shape from a flat surface such as a residual tilt, curvature and cylinder are numerically removed from the areal measurement producing a surface topography map. Further filtering may be applied to the surface topography map as required.

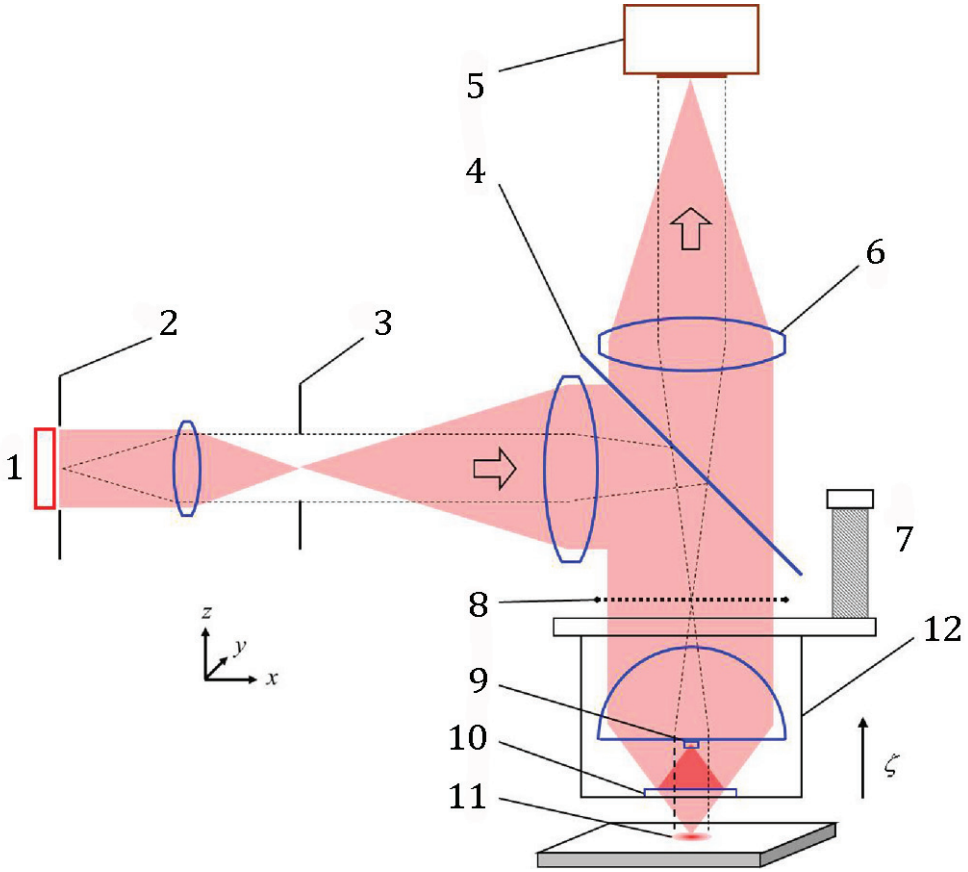

Key

1	light source	7	scanner
2	aperture stop	8	pupil plane
3	field stop	9	reference mirror
4	illumination beamsplitter	10	interferometer beamsplitter
5	camera	11	object surface
6	tube or zoom lens	12	Mirau interference objective

NOTE Other configurations are listed in A.4.

Figure A.1 — Schematic diagram of a typical Mirau-configuration CSI microscope

A.2 Typical configuration

Figure A.1 illustrates the basic features of a CSI microscope. The object has height features h which vary over the object surface. A mechanical scanner provides a smooth, continuous scan ζ of the interference objective in the z direction. During the scan, a computer records intensity data, $I(\zeta)$, for each image point or camera pixel x, y in successive camera frames.

A.3 Light source

A distinctive feature of CSI is that the light source is generally incoherent. Thus, typical light sources either have a broadband spectrum (white light) or are extended (many independent point sources), or both. A classic example is an incandescent lamp such as a tungsten halogen bulb. Solid state sources, such as light emitting diodes (LEDs) are increasingly common. They may emit white, green, blue, or infrared light.

The illumination optics as shown in Figure A.1 typically images the light source into the pupil of an interference objective (Köhler illumination). The aperture stop controls the illumination A_N (numerical aperture, see 2.3.6), while the field stop controls the size of the object surface that is illuminated. For dynamically-moving objects such as oscillating micro structures, the light source may be flashed at high speed to stroboscopically freeze the object motion, see References [19] and [20].

A.4 Interference objective

CSI instruments, like phase-shifting interferometry microscopes, are most often configured in a manner similar to a conventional microscope with the normal objective replaced by a two-beam interference objective. Interference objectives are most commonly of the Michelson, Mirau, or Linnik type, see Reference [21]. Some systems for larger fields of view use the Twyman Green geometry (Figure A.2), see References [6] and [22].

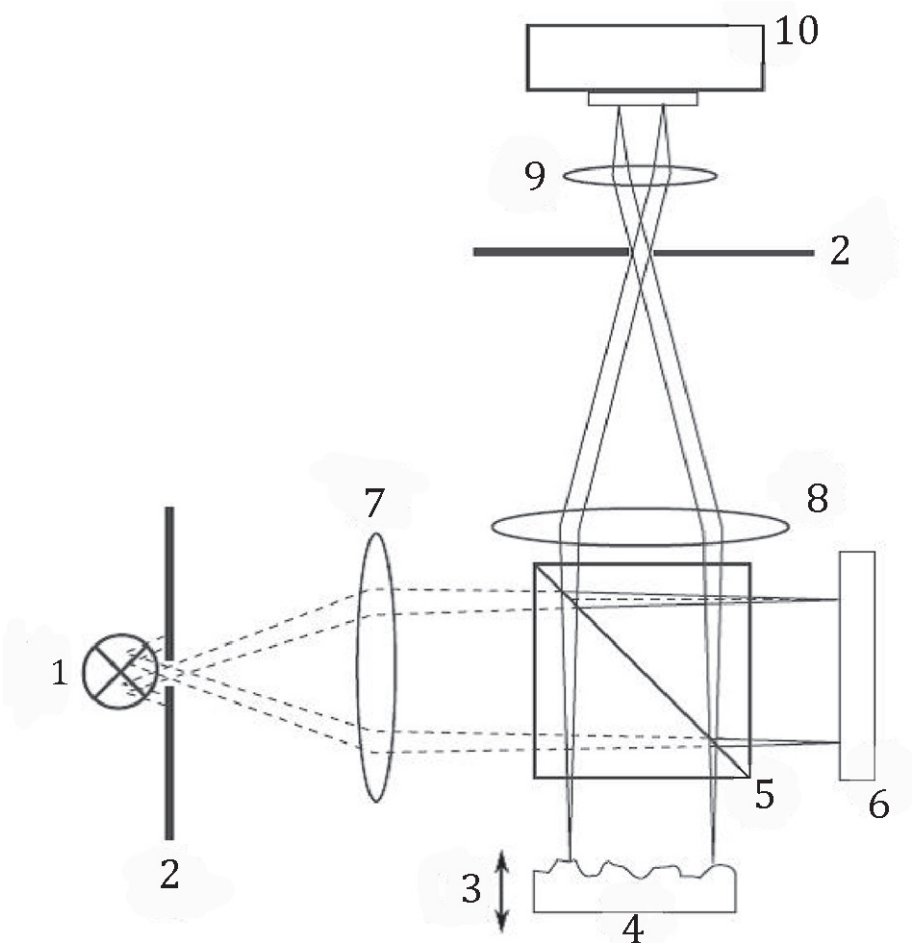

Key

1	light source	6	reference flat
2	aperture	7	condenser
3	*z*-positioning	8	object lens
4	specimen	9	camera lens
5	beamsplitter	10	camera

Figure A.2 — Optical principle of a Twyman-Green-interferometer with camera sensor

Because the objective is scanned, the objective is preferably optimized to operate as an *infinite conjugate* lens, meaning that a point on the object is imaged at infinity. The system magnification is the ratio of the tube lens focal length (Figure A.1) to the focal length of the objective. The objective magnification

is defined in terms of a nominal unity-magnification tube lens focal length, which varies between 160 and 200 mm, depending on the manufacturer. Thus, a 10X objective for a defined 200 mm tube lens has a focal length of 20 mm.

Microscope objectives generally have a larger A_N with increasing magnification, which influences the interferometer design. As defined in 2.3.6 and shown in Figure 2, the A_N is equal to n sin α. The environment in a CSI instrument is usually air; therefore, the index n is close to 1. The sine of the angle α is equal to the pupil radius divided by the objective focal length.

Another important characteristic of an interference objective is the working distance, which as illustrated in Figure A.3, is the distance from the objective housing to the object. The working distance is a function of the design of the objective, and relates to factors such as interferometer geometry, focal length, mechanical structure and lens design. A large working distance is generally preferred and can be a deciding factor in the choice of interferometer geometry. For magnifications of 10X and smaller, for example, the Michelson interferometer using a prism beamsplitter is widely used because it is easy to manufacture, has no obscurations and provides adequate working distance. The Twyman Green interferometer, e.g. allows for a large working distance and a large scanning range. At higher magnifications, the Mirau geometry is more prevalent because it provides a greater working distance. For the highest magnifications, the Linnik is sometimes chosen because it has the largest working distance for a given lens design than all other geometries.

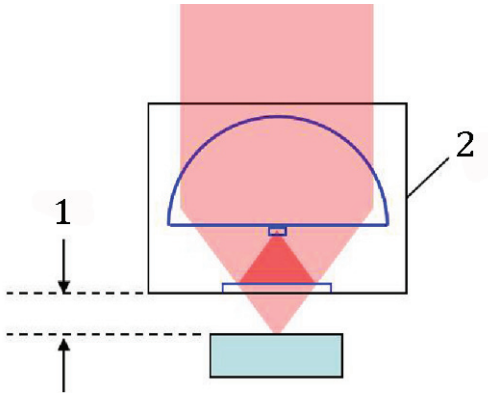

Key

1 working distance

2 objective housing

Figure A.3 — Illustration of working distance

In all cases, the interference objective for a CSI instrument must be compatible with a low-coherence light source, meaning in part that the position of best focus should be coincident with the position of zero optical path difference, and the two interferometer paths should be balanced for dispersion of refractive index with wavelength. In some cases, where the object surface may be underneath glass or a layer of liquid, it is beneficial to introduce a dispersion compensation element into the reference path, see Reference [23]. In addition, the amplitude modulation (see 2.5.6) and signal to noise ratio are optimized when the backreflected intensities from the reference arm and the object arm are almost equal. This can be achieved either by using an objective with reference surface reflectivity matched to the surface or by inserting neutral density filter in one of the arms.

For some applications, a nonflat reference surface may be used that better matches the sample shape. For example, measurement of the surface topography of a curved surface may be optimized with a spherically-shaped reference surface, see Reference [24].

A.5 Scanner

The scanner shown in Figure A.1 moves the interference objective or the objective turret; in other cases the object moves. Generally, the scan motion is along the optical axis of the objective perpendicular to the sample surface, i.e. in the z -direction, as shown in Figure A.1. The scan length of the CSI scanner is typically between 10 µm and 200 µm for piezoelectric scanners. For motorized scanners, the scan length may be up to 70 mm, see Reference [25]. A constant scanner motion or accurate knowledge of the scanner position obtained by a position feedback system is important to the overall accuracy of the CSI instrument, as discussed in B.4. Although less common, it is feasible to move the reference mirror, beam splitter or some combination of optical elements within the objective in place of translating the entire interference objective.

A.6 Camera

Most CSI systems generate 3D surface topography maps using an electronic detector comprised of a 2D array of pixels. However, 2D profiles made using 1D linear detectors also are feasible but are less common in modern commercial instruments.

Annex B
(informative)

Coherence scanning interferometry (CSI) theory of operation

B.1 Concept

Figure B.1 shows the image as viewed by the camera in Figure B.2 for three successive scan positions. The concentric-ring interference patterns for this convex curved object progress from the outside to the inside as the interference objective scans upward. The localization of the interference fringes allows one to determine the height of the object surface by e.g. identification of the scan position corresponding to the passage of the highest-contrast fringe at each pixel in the field of view.

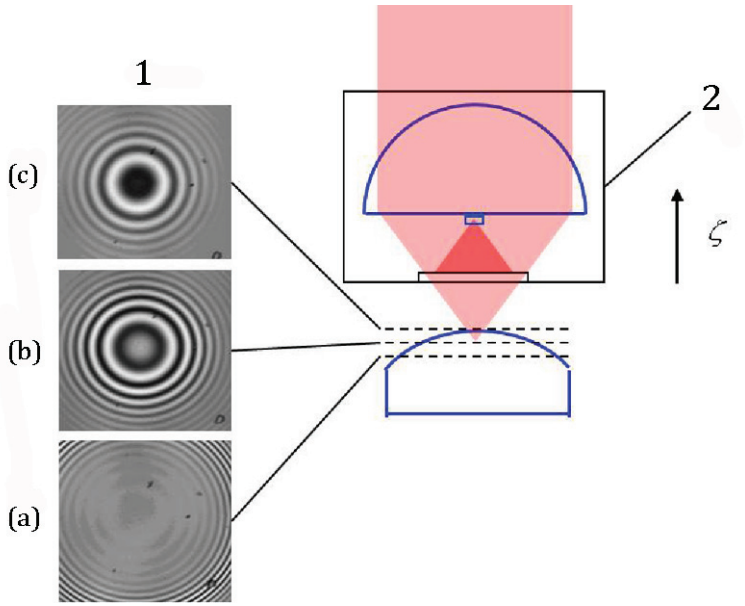

Key

1 images

2 interference objective

Figure B.1 — Conceptual drawing of the operation of a CSI instrument, showing the interference fringe pattern on a curved object for three different successive scan positions (a), (b), (c)

B.2 Signal generation

B.2.1 Incoherent superposition

A simplified model of signal generation assumes a randomly-polarized, spatially incoherent illumination and a smooth surface perpendicular to the incident light beam that does not scatter or diffract incident light, see References [2], [6] and [26]. The total signal is the sum of all the incoherent interference contributions of the ray bundles passing through the pupil plane of the objective and reflecting from the object and reference surfaces.

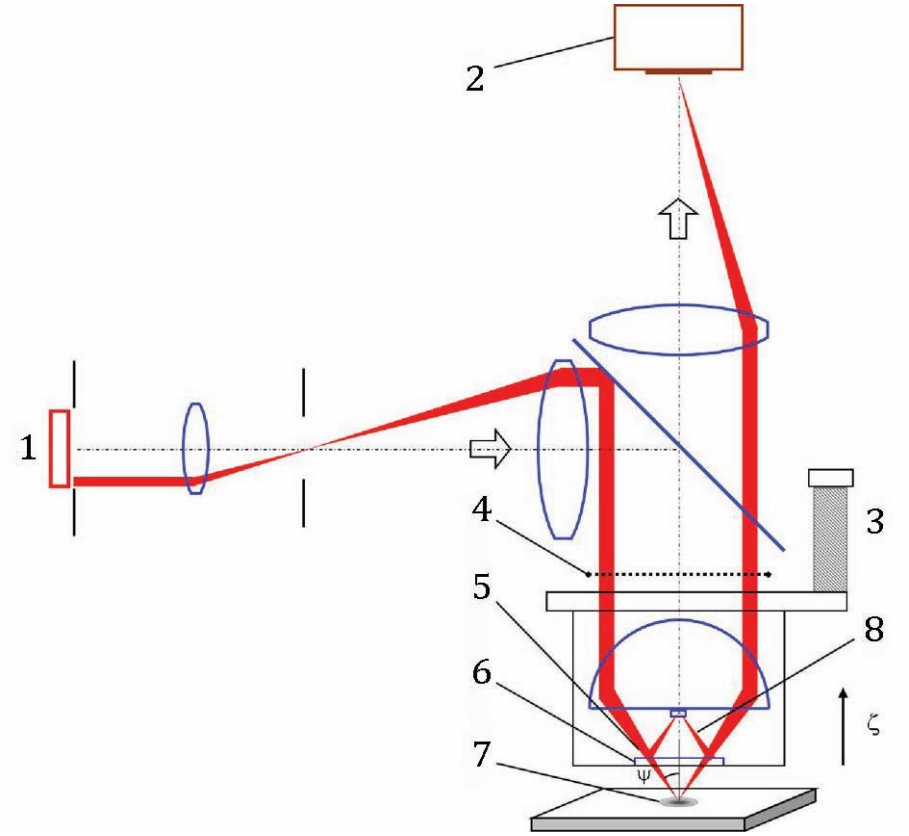

Key

1	light source	5	ray incident at incident angle Ψ
2	camera	6	interferometer beamsplitter
3	scanner	7	object surface
4	pupil plane	8	reference path

Figure B.2 — CSI microscope showing the path of a single ray bundle for a specific source point and image point, incident on the object surface at an angle Ψ

For example, the ray bundle at an incident angle Ψ shown in Figure B.2 corresponds both to a specific image point (x', y') and to a specific position in the pupil. This ray bundle is divided at the beam splitter into a bundle following the measurement path to the object surface at a particular point (x, y) and a bundle following a reference path to the reference mirror. ζ is the scan position of the surface with respect to the microscope, and the interference fringe spatial frequency is

$$K = 4\pi\frac{\beta}{\lambda} \tag{B.1}$$

for a directional cosine $\beta = \cos(\Psi)$ and a wavelength λ.

The summation over a range of frequencies results in a peak signal strength where all of the individual contributions are mutually in phase. This position is sometimes referred to as the stationary phase point and corresponds to the peak of the envelope shown in Figure B.3. The incoherent superposition model allows for mathematical prediction of signal shape and is useful for evaluating software means for determining surface heights from the CSI signal, see References [27] and [28].

B.2.2 Limit case: white light and low A_N

Certain simplifying limit cases are of practical and conceptual value. A familiar configuration is low A_N with broadband or "white" light, for which Figure B.3 is a typical interference signal. The spectral

distribution for this shape is shown in Figure B.4 and is directly proportional to the source spectral distribution. Therefore, there is a Fourier transform relationship between the interference signal and the emission spectrum of the white light source.

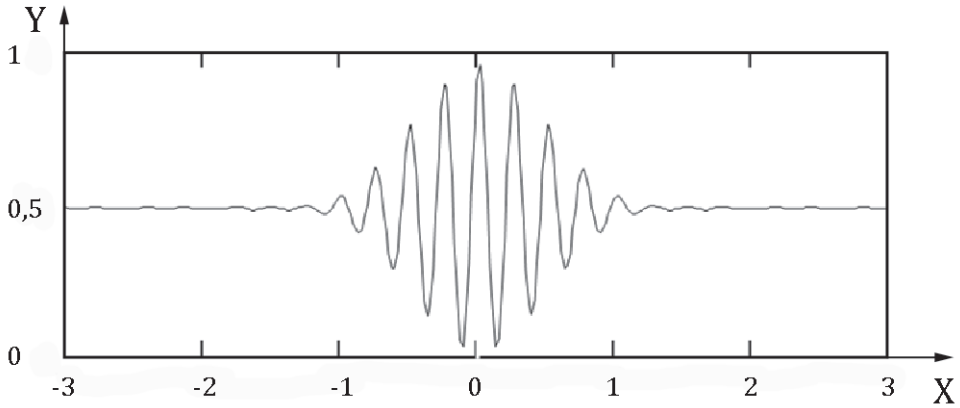

Key

X scan position ζ (µm)

Y intensity

NOTE The broad spectral bandwidth of the light source results in a modulation envelope that localizes the interference fringes about the zero scan position (see Figure 3).

Figure B.3 — White light interference signal simulation

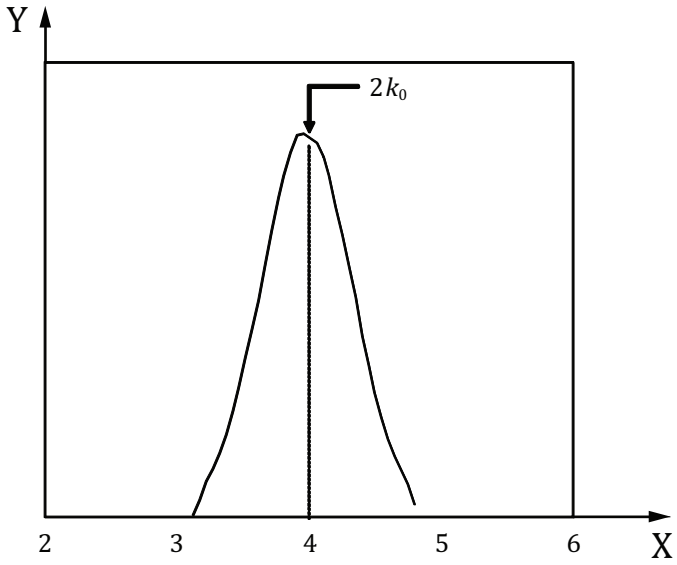

Key

X interference signal spatial frequency (cycles/μm)

Y Fourier magnitude

NOTE Here, k_0 = 2π/500 nm and one cycle = 2π. The range of frequencies is the result of the spectral bandwidth of the light source.

Figure B.4 — Fourier magnitude of the interference signal (Figure B.3) for a low A_N system of 0,2 illuminated by a 100 nm bandwidth white light source centred at 500 nm

B.2.3 Limit case: Narrow bandwidth and high A_N

A somewhat less familiar but no less relevant case is narrow bandwidth at high A_N. Now the frequency spectrum (Figure B.6) and interference signal (Figure B.5) are shaped by the light distribution in the pupil plane, rather than by the spectrum of the light source, which is assumed to be monochromatic with a single wavenumber $k_0 = 2\pi/\lambda_0$. Although not strictly speaking a white light interferometer, a high-A_N monochromatic system nonetheless creates similar signals and functions in much the same way as a white light instrument.

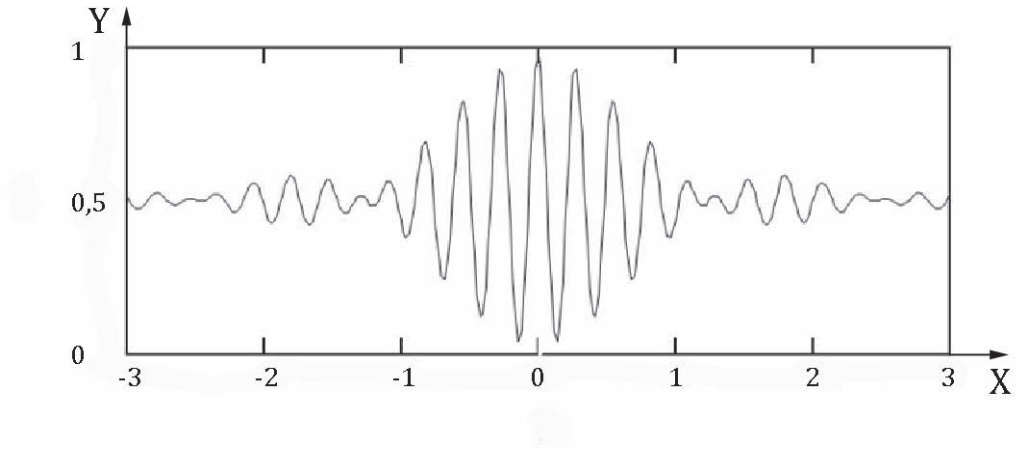

Key

X scan position (μm)

Y intensity

NOTE The modulation envelope is the result of the high A_N and spatially incoherent illumination.

Figure B.5 — High A_N monochromatic interference signal simulation

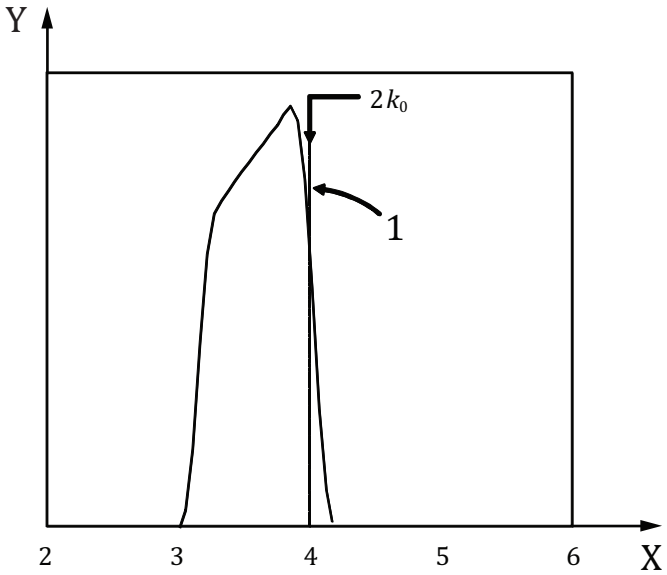

Key

X interference signal frequency (cycles/μm)

Y Fourier magnitude

1 normal incidence limit

NOTE The high A_N results in multiple angles of incidence having varying frequencies for contributions to the interference signal. Here, $k_0 = 2\pi/500$ nm and one cycle = 2π.

Figure B.6 — Fourier magnitude of the interference signal (Figure B.5) for a narrow 20 nm bandwidth source uniformly filling a wide, 0,6-A_N pupil (approximately 50X magnification)

In practice, CSI microscopes operate in a compromise regime, wherein both spatial coherence and spectral bandwidth contribute to the signal shape. Typically, the low-A_N, white light condition is approximately satisfied when using objectives with magnification of 5X or lower; while for a magnification of 50X or higher focus effects contribute strongly to signal shape.

B.3 Signal processing

CSI signals are qualitatively characterized by rapidly-oscillating interference fringes and an overall variation in signal strength, which localizes the interference effect to a specific value of ζ. In some specific cases, such as an unstructured surface, $h_{x,y}$, a symmetric white light spectrum and low A_N, the interference signal $I_{x,y}(\zeta)$ (Figure B.3) is mathematically separable into a constant offset I_0 and a co-sinusoidal *carrier* signal at a spatial frequency K_0 modulated by a slowly-varying I_{AC} *modulation envelope*, approximately as

$$I_{x,y}(\zeta) = I_0(\zeta) + I_{AC}(\zeta - h_{x,y})\cos\left[K_0(\zeta - h_{x,y})\right] \quad \text{(B.2)}$$

For systems with higher A_N, as a result of spatial coherence effects, the shape of the envelope is a function of both the optical path difference and focus effects.

Real CSI signals are generally more complicated than an envelope-modulated carrier; nonetheless, the basic concept of a signal envelope has practical utility in the development of signal processing strategies. For this reason, the development of automated techniques for three-dimensional measurement of surface topography using CSI began in the 1980s with various techniques for electronic envelope detection, see References [29] and [30].

Many CSI microscopes offer an enhanced analysis mode that couples envelope detection of the fringe order with the much finer resolution of estimating the interference phase to improve the precision of CSI on surfaces that are smooth (e.g. < λ/10 rms surface roughness). An approach to simultaneous envelope detection and phase analysis is to correlate the measured intensity data at each pixel with a complex kernel function designed to be sensitive to the CSI signal, see Reference [31]. Alternatively, one can analyse the CSI signal by directly examining its frequency content in the Fourier transform domain, see Reference [32].

The various detection methods are effective for measuring surface topography maps on both smooth and rough surfaces but may suffer from sensitivity to error sources to a much greater degree than conventional interference phase techniques such as phase shifting interferometry, see Reference [33]. Some errors in the evaluation are evident as errors in the fringe order evaluation and are sometimes called 2π errors. These are most common with surfaces having differing optical properties across the field of view, film structures, sharp edges, or high surface roughness. Considerable effort has been dedicated to a proper treatment of the fringe-order and it remains a central point of software development for CSI, see References [10], [34] and [35].

B.4 Determination of vertical displacement for CSI

In CSI, unlike other interferometric techniques, the wavelength of light does not define the height scale. Because the interferometric pattern is used as a surface sensor only, the basic unit of measure is defined by the *scan increment*, rather than the wavelength of light, see Reference [36]. Conceptually, a CSI instrument behaves like a highly parallel, optical contact probe. The software records the location of the CSI signal at each pixel with respect to a scan position, resulting in a surface topography map, the scale and linearity of which are directly tied to knowledge of the scan motion.

The metrology remains tied to the scan increment even when incorporating interference phase to improve the precision of CSI measurements. This is a consequence of requiring that the envelope detection and phase estimation measurements agree in scale in order to combine them into a final result, see Reference [37], which is complicated by such effects as the objective A_N, which influences the effective wavelength, see Reference [26]. A frequency domain analysis, see Reference [32], post-processing of

the CSI signals, see Reference [12] or a setup calibration procedure may be used to calibrate the phase measurement with respect to the scan increment.

Given that CSI measurement relies on knowledge of the scan motion, some instruments equip the scanner with electronic sensors such as capacitance sensors, linear variable differential transformers (LVDTs), displacement interferometers, see References [20] and [38], optical encoders, or other methods used in feedback systems to improve scan linearity.

B.5 Dissimilar materials

The optical properties of the materials that make up the object surface are integral to the measurement process. In particular, assuming that the material has an index of refraction with at most a linear dispersion in wavenumber ($2\pi/\lambda$), one can identify, see References [35] and [39]:

— a phase change on reflection (PCOR) that influences the measured interference fringe phase, and

— a rate of change of PCOR or *PCOR dispersion*, which influences the position of the modulation envelope.

If the object surface material is uniform, there is generally no resulting identifiable error in the final surface topography map, assuming that an overall DC offset is irrelevant. For surfaces composed of a mixture of materials having different optical properties, errors in topography measurement can be introduced because of the differences in the phase shift upon reflection. Even thin non-uniform oxides can cause significant variations in the phase change upon reflection across the surface. These errors may in principle be corrected using *a priori* knowledge of the PCOR and rate of change of PCOR, see Reference [16].

Table B.1 quantifies the metrology effects of PCOR and PCOR dispersion for a few common materials. Note that there is no simple correlation between the envelope shift and the phase shift, which in practice means that it is difficult to develop a strategy for determining the PCOR *in situ* without further information. The observed height shifts depend as well on the A_N of the objective, in a manner which can be determined by detailed signal modelling, see Reference [16].

Table B.1 — Change in apparent surface height resulting from PCOR (phase shift) and the rate of change of PCOR (envelope shift), for a 570 nm light source with a 100 nm bandwidth, at low A_N

Material	Envelope shift nm	Phase shift nm
Bare glass	0	0
Silicon	–3	0
Aluminium	–9	–13
Chrome	–15	–13
Platinum	–11	–18
Copper	–1	–31
Cobalt	–11	–18

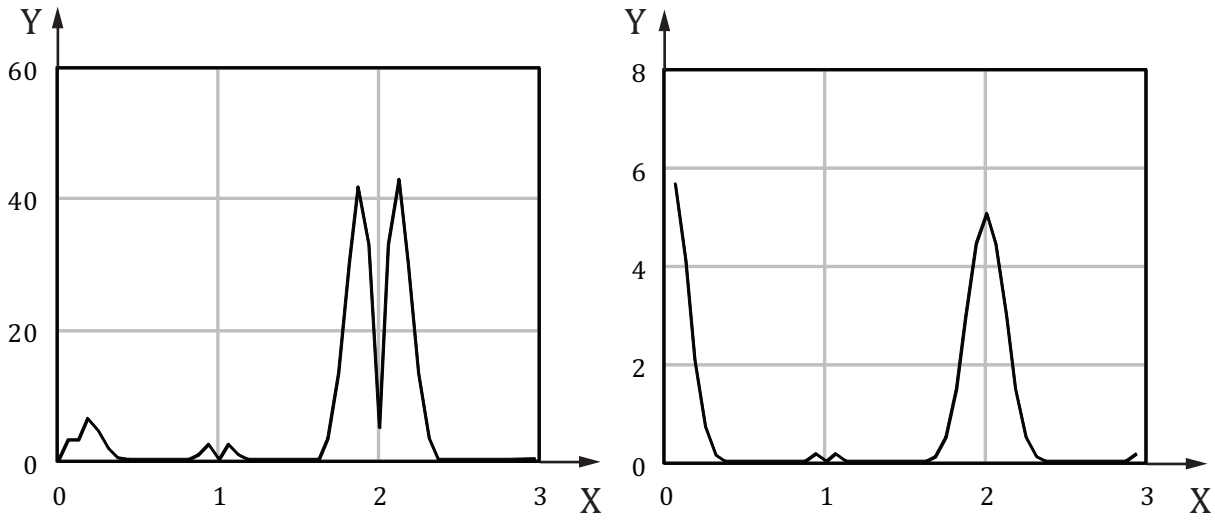

Key

X vibrational frequency/fringe rate

Y rms error (nm)

NOTE Left-hand graph is for envelope detection, right-hand graph is for interference phase. For these simulated data, the 560 nm light source has a 120 nm bandwidth.

Figure B.7 — Sensitivity of CSI to a 10 nm amplitude sinusoidal mechanical vibration as a function of vibrational frequency, see Reference [28]

B.6 Vibrations

CSI measurements acquire data over time, which means that other time-dependent phenomena, such as mechanical vibrations, tend to be convolved into the data. The environment can therefore be an important contributor to measurement error.

Figure B.7 shows the sensitivity of CSI to vibration as a function of frequency, normalized to the interference fringe scan rate, see Reference [28] (for example, 10 Hz vibration at a scan rate such that 5 interference fringes pass per second would be a normalized frequency of 2). The very high sensitivity of envelope detection to vibration, approximately 10 times greater than for phase measurement, mandates that the CSI tool be situated in an environment isolated from sources of vibration, particularly at a normalized frequency of 2.

In some cases of practical interest, high measurement errors related to stable, single-frequency vibrations can be reduced by altering the scan rate to avoid the peak sensitivities evident in Figure B.7.

B.7 Films

One of the unique benefits of CSI recognized early in its development is the ability to separate multiple reflections from semi-transparent film structures on surfaces, see References [4], [5] and[40]. From Figure B.8, it is apparent that for a sufficiently thick single-layer film, there are two clearly identifiable modulation envelopes corresponding to surface reflections from the film boundaries. Therefore, an approach to generating surface topography maps over films is to identify the right-most signal as the top surface signal, as shown in Figure B.8. Further, if the refracting properties of the film are known, the substrate or other secondary surfaces below the top surface can be mapped for height by analysis of the signals that follow the top-surface signal, yielding additional information such as 3D film thickness

maps. Alternatively, if the physical thickness of a film layer is known, the refracting properties of the film material may be determined by analysis of the CSI signal.

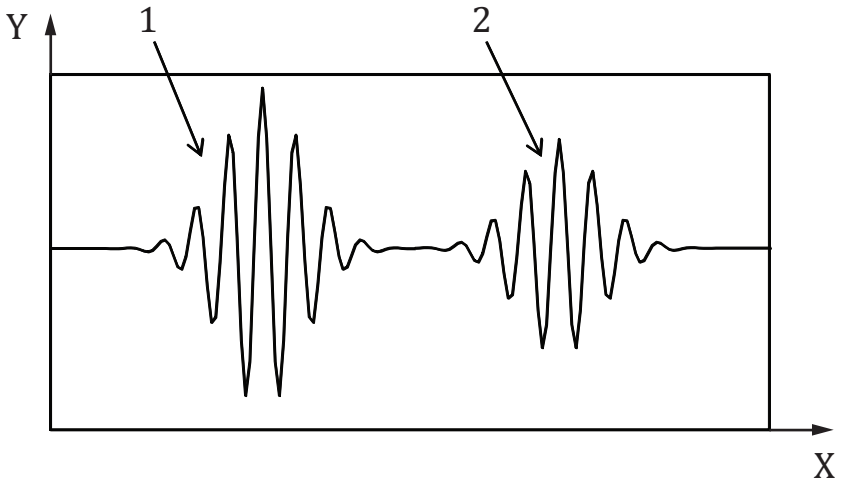

Key

X	scan position	1	substrate signal
Y	intensity	2	top surface signal

Figure B.8 — CSI signal in the presence of a single-layer transparent film a few micrometres in thickness

A caution when analysing film thickness maps is that the location of the substrate or secondary-surface signal is influenced by two competing effects: the axial group-velocity optical path length, which is longer in a film than in air, and the position of best focus, which is shorter in a film than in air. These two competing effects strongly influence the shape and position of CSI signals resulting from reflections within a film, see Reference [16].

If the film is too thin, the separate signals shown in Figure B.8 coalesce and it is difficult to clearly separate them. The film thickness at which separation becomes difficult depends on the coherence length of the measurement light in the thin film and is roughly several µm. Depending on the instrument configuration, there is a lower limit to an analysis based entirely on signal separation, below which some level of modelling becomes necessary to interpret the CSI signal.

B.8 Missing data and bad data

Some places on the surface may not be measurable because of a low signal to noise ratio. These may be regions of high slope or places where surface irregularities are present. If the measurement algorithm identifies these places, they may be classified as *missing data* or *dropouts*. Alternatively, measurement of such regions may result in *bad data* or *outliers*, which fail to be identified but which can lead to erroneous results when the surface is analysed for parameters. Supplementary statistical algorithms can be used to identify these bad data points. Surfaces can then be analysed for parameters by excluding the bad and missing points or by interpolating through the bad and missing data points.

Annex C
(informative)

Spatial resolution

C.1 Instrument transfer function

An informative method of describing the spatial (lateral) resolving power of CSI microscopes is by the instrument transfer function [ITF or $f_{\mathrm{ITF}}(\nu)$], see References [41] and [42]. The ITF is the equivalent for topography measuring instruments of the optical transfer function (OTF) [ISO 9334:2012, 3.8] for conventional microscopes. The ITF describes how the instrument would respond to an object surface having a specific spatial frequency. Ideally, the ITF tells us what the measured amplitude of a sinusoidal grating of a specified spatial frequency ν (e.g. in lines/mm) would be relative to the true amplitude of the grating. The ITF also affects the value of the S-filter, which has to be applied in order to avoid data artefacts, such as that due to high frequency noise (see ISO 25178-3:2012, 4.2.3). It is assumed for simplicity here that the surface is rough along the x-direction and is described by the function $h(x)$. Because the surface structure may be represented as a sum of spatial frequency components by a Fourier transform (F), the surface will have a *measured* height profile $h'(x)$ given by

$$h'(x) = \mathrm{F}^{-1}G'(\nu), \tag{C.1}$$

where F^{-1} is the inverse Fourier transform,

$$G'(\nu) = f_{\mathrm{ITF}}(\nu)\, G(\nu), \tag{C.2}$$

and

$$G(\nu) = \mathrm{F}\, h(x) \tag{C.3}$$

In the limit of very small surface heights, the ITF of a CSI instrument having an incoherent light source that fills the objective pupil is given by

$$f_{\mathrm{ITF}}(\nu) = \tfrac{2}{\pi}\left[\phi - \cos(\phi)\sin(\phi)\right] \tag{C.4}$$

where

$$\phi = \arccos\left(\frac{\lambda\nu}{2A_N}\right) \tag{C.5}$$

To fully characterize the instrument, this ITF [Formula (C.4)] must be multiplied by the modulation transfer function (MTF) of the camera, whose resolution is limited by the pixel size. Figure C.1 shows theoretical ITFs for CSI microscopes with several objectives and also including the MTF of a certain camera.

Setting aside the contribution of the camera resolution, the ITF reaches zero for a spatial frequency given by $\phi = 0$ or

$$v_{0\%} = \frac{2A_N}{\lambda}\,, \tag{C.6}$$

which is nearly equal to the *Sparrow criterion* for optical resolution. The 50 % point is at

$$v_{50\%} = \frac{A_N}{1,22\lambda} \tag{C.7}$$

which is half the spatial frequency (twice the spatial period) of the *Rayleigh criterion*, see References [43] and [44]. Table C.1 summarizes the optical lateral resolution for common CSI objectives in terms of these two criteria.

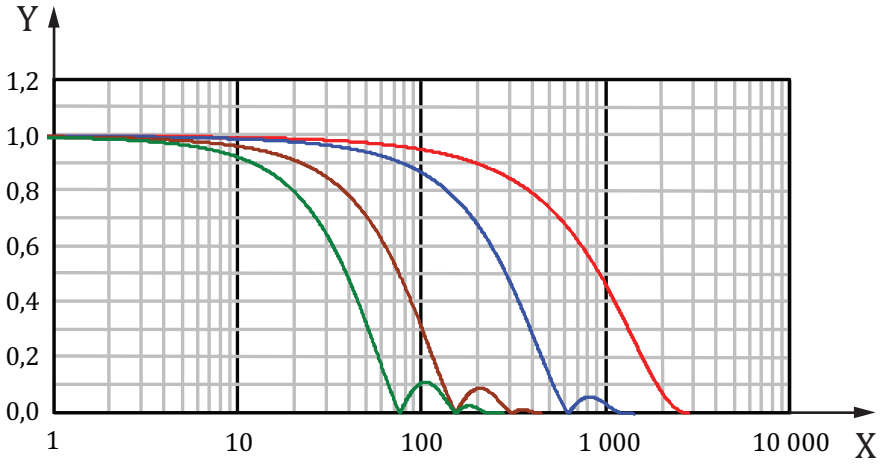

Key

X spatial frequency (cycles/mm)

Y instrument transfer function

Figure C.1 — Magnitude of the theoretical ITF for 2,5X, 5X, 20X and 100X microscope objectives (A_N equal to 0,075, 0,13, 0,3, 0,8, respectively), with higher magnifications to the right, including the effect of a 640 × 480 pixel camera with a 1X tube lens

Table C.1 — Topographic spatial resolution of common CSI objectives, assuming perfect optics and excluding the effects of the camera, calculated for a wavelength of 550 nm

		Topographic spatial resolution	
Magnification	A_N	**Rayleigh** µm	**Sparrow** µm
1×	0,03	11,18	8,62
2,5×	0,08	4,19	3,23
5×	0,13	2,58	1,99
10×	0,30	1,12	0,86
20×	0,40	0,84	0,65
50×	0,55	0,61	0,47
100×	0,80	0,42	0,32

It is essential to realize that simply having a particular A_N does not mean that the objective will perform as tabulated in Table C.1. Aberrations or variations in the illumination can strongly influence the actual performance of the instrument.

Between the two criteria, only the *Rayleigh criterion* (2.3.7) can be validated directly by an experimental measurement of instrument response to the 50 % level. Therefore, it is the preferred specification. If the *Sparrow value* (2.3.8) is cited, it can be validated by determining first the Rayleigh criterion value and then multiplying by 0,77.

Camera resolution is usually matched to the optical resolution up to approximately 10X, meaning that the pixel size in object space has the same lateral dimensions as listed in Table C.1. Above 20X, the camera resolution exceeds the optical resolution, becoming a negligible limit on the net ITF at 100X, as is apparent from Figure C.1.

A caution regarding the ITF is that it is theoretically valid only in the regime of surface heights much smaller than the wavelength. In addition, higher spatial frequencies can cause artefacts in the results, see Reference [45].

Features with larger height variations can have unexpected results, including sensitivity to spatial frequencies beyond the Sparrow criterion, because of nonlinear coupling, see References [41] and [46]. A further caution is that the ITF calculation is based on a scalar Abbe theory, whereas a more rigorous vector solution of Maxwell's equations may lead to different results, particularly at high A_N. These cautions noted, in general practice the ITF curves such as those in Figure C.1 are useful predictors of instrument function.

C.2 ITF measurement

Procedurally, the ITF may be calculated directly by comparison of the spatial frequency content of a measured surface topography map divided by the theoretical spatial frequency content of the object surface. A convenient object for this comparison is a step height of no more than one-eighth the mean source wavelength in height, see Reference [41]. Figure C.2 shows one such profile for a nominally 40 nm step. The ratio of the Fourier transform of these two plots yields the ITF, as illustrated in Figure C.3.

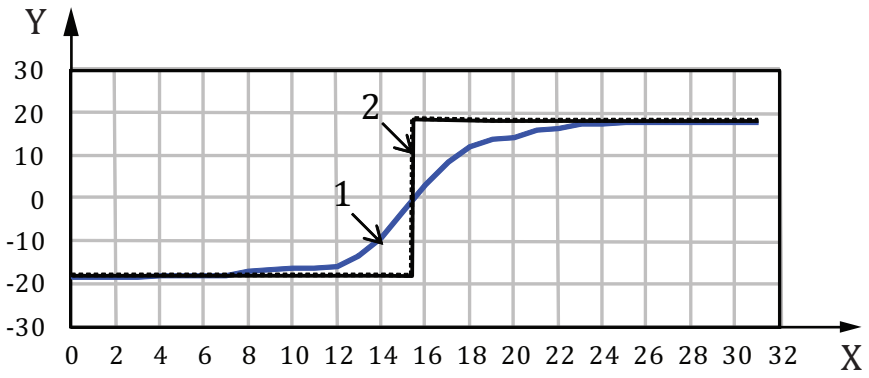

Key

X	lateral coordinate (pixel)	1	output data
Y	height (nm)	2	perfect step

Figure C.2 — Comparison of the measured profile of a step with a theoretically perfect step

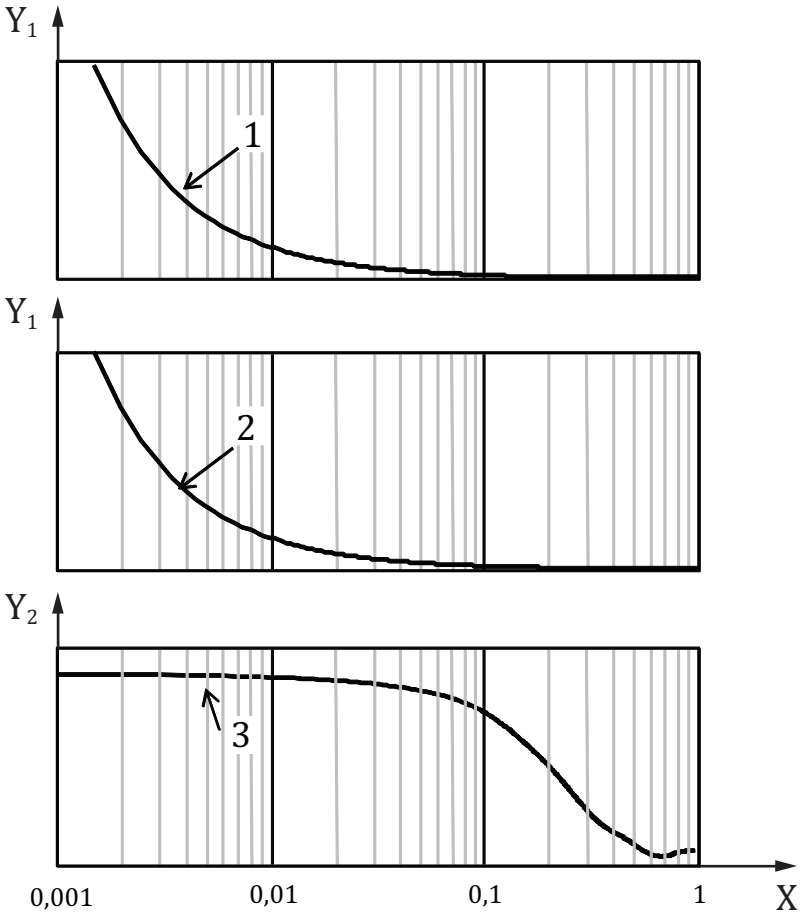

Key

X	spatial frequency (Nyquist = 1)	1	Fourier transform of measured step
Y_1	Fourier magnitude	2	Fourier transform of perfect step
Y_2	relative magnitude	3	ratio C/D

NOTE The spatial frequency in this graph is normalized to the Nyquist sampling frequency, which is half the spatial frequency (twice the spacing) of the camera pixels.

Figure C.3 — Illustration of a process for experimentally determining the ITF using step-profile data

Annex D
(informative)

Example procedure for estimating surface topography repeatability

CSI instruments report various measurands such as peak-to-valley, rms roughness, step height and so on, all of which are derived from a topography image of surface heights. Surface topography repeatability, defined in 2.1.11, provides the likely agreement between repeated measurements. For instrument benchmarking and performance validation, surface topography repeatability is usually performed on an optically smooth surface. The conditions and parameters for the surface topography repeatability measurement must be described.

The following procedure has been used for estimating the surface topography repeatability.

a) Acquire a number n of measurement maps (for example, 10) without averaging or lateral smoothing and remove from each individual map a least-squares plane such that each resulting map $(h_{x,y})_{1,2,..n}$ has zero mean height and zero tilt.

b) Create an average map. $\langle h_{x,y} \rangle$

c) Subtract the average map $\langle h_{x,y} \rangle$ from each individual map $(h_{x,y})_{1,2,..n}$ and record the root-mean-square value $\varepsilon_{1,2,...n}$ for each difference map over all pixels.

d) The surface topography repeatability is the arithmetic mean value of the population of values $\varepsilon_{1,2,...n}$.

The scan increment (often 4 camera frames per interference fringe for CSI) and any relevant environmental conditions should be clearly noted.

Annex E
(informative)

Relation to the GPS matrix model

E.1 General

For full details about the GPS matrix model, see ISO/TR 14638.

The ISO/GPS Masterplan given in ISO/TR 14638 gives an overview of the ISO/GPS system of which this document is a part. The fundamental rules of ISO/GPS given in ISO 8015 apply to this document and the default decision rules given in ISO 14253-1 apply to specifications made in accordance with this document, unless otherwise indicated.

E.2 Information about this part of ISO 25178 and its use

This part of ISO 25178 defines the basic terminology and metrological characteristics for non-contact (coherence scanning interferometric microscopy) instruments.

E.3 Position in the GPS matrix model

This part of ISO 25178 is a general GPS standard, which influences chain link 5 of the chains of standards on roughness profile, waviness profile, primary profile and areal surface texture in the general GPS matrix, as illustrated in Table E.1.

Table E.1 — Fundamental and general ISO GPS standards matrix

		Global GPS standards						
		General GPS standards						
		Chain link number	**1**	**2**	**3**	**4**	**5**	**6**
Fundamental GPS standards		Size						
		Distance						
		Radius						
		Angle						
		Form of line independent of datum						
		Form of line dependent on datum						
		Orientation						
		Location						
		Circular run-out						
		Total run-out						
		Datums						
		Roughness profile					•	
		Waviness profile					•	
		Primary profile					•	
		Surface defects						
		Edges						
		Areal surface texture					•	

E.4 Related International Standards

The related International Standards are those of the chains of standards indicated in Table E.1.

Bibliography

[1] ISO/IEC Guide 99:2007, *International vocabulary of metrology — Basic and general concepts and associated terms (VIM)*

[2] WYANT. JC and Schmit, J. Large Field of View, High Spatial Resolution, Surface Measurements. *Int. J. Mach. Tools Manuf.* 1998, **38** (5-6) pp. 691–698

[3] WINDECKER. R, Haible, P and Tiziani, HJ. Fast coherence scanning interferometry for measuring smooth, rough and spherical surfaces. *J. Mod. Opt.* 1995, **42** (10) pp. 2059–2069

[4] DAVIDSON. M, Kaufman, K, Mazor, I and Cohen, F. An application of interference microscopy to integrated circuit inspection and metrology. *Proc. SPIE*. 1987, **775** pp. 233–247

[5] LEE. BS and Strand, TC. Profilometry with a coherence scanning microscope. *Appl. Opt.* 1990, **29** (26) pp. 3784–3788

[6] DRESEL. T, Haeusler, G and Venzke, H. Three-dimensional sensing of rough surfaces by coherence radar. *Appl. Opt.* 1992, **31** (7) pp. 919–925

[7] LEE-BENNETT, I. Advances in non-contacting surface metrology. *Optical Fabrication and Testing, OTuC1,* 2004, Rochester, October 11-13.

[8] KINO. GS and Chim, SSC. Mirau correlation microscope. *Appl. Opt.* 1990, **29** (26) pp. 3775–3783

[9] LARKIN. KG. Efficient nonlinear algorithm for envelope detection in white light Interferometry. *J. Opt. Soc. Am. A Opt. Image Sci. Vis.* 1996, **4** pp. 832–843

[10] WYANT, JC.. How to extend interferometry for rough-surface tests. *Laser Focus World,* September 1993, pp. 131-135

[11] CONNOLLY, T.. Scanning interferometer characterizes surfaces. *Laser Focus World,* August 1995, p. 84.

[12] SCHMIT. J and Olszak, AG. Some challenges in white light phase shifting Interferometry. *Proc. SPIE*. 2002, **4777** p. 118

[13] SCHMIT, J and CHEN, D.. Greater Measurement Detail with High-Definition Vertical Scanning Interferometry. *Veeco Instruments Inc. Applications Note AN541*.

[14] CABER. PJ.. Interferometric profiler for rough surfaces. *Appl. Opt.* 1993, **32** (19) pp. 3438–3441

[15] WYKO RST (Rough Surface Tester). *Wyko Corporation product literature*. Tucson, Arizona, 1992

[16] de GROOT. P and Colonna de Lega, X. Signal modeling for low coherence height-scanning interference microscopy. *Appl. Opt.* 2004, **43** (25) p. 4821

[17] de GROOT, P, Biegen, J, Clark, J, Colonna de Lega, X and Grigg, D. Optical interferometry for measuring the geometric dimensions of industrial parts. *Appl. Opt.* 2002, **41** (19) pp. 3853–3860

[18] WAN, D-S, Schmit, J and Novak, E. Effects of source shape on the numerical aperture factor with a geometrical-optics model. *Appl. Opt.* 2004, **43** (10) pp. 2023–2028

[19] NAKANO, K, Yoshida, H, Hane, K, Okuma, S and Eguchi, T. Fringe scanning interferometric imaging of small vibration using pulsed laser diode. *Trans. of SICE*. 1995, **31** (4) pp. 454–460

[20] NOVAK, E, Krell, MB and Browne, T. Template-based software for accurate MEMS characterization. *Proc. SPIE*. 2003, **4980** pp. 75–80

[21] ISO 25178-603, *Geometrical product specifications (GPS) — Surface texture: Areal — Part 603: Nominal characteristics of non-contact (phase-shifting interferometric microscopy) instruments*

[22] DE GROOT. P, Colonna de Lega, X and Grigg, D. Step height measurements using a combination of a laser displacement gage and a broadband interferometric surface profiler. *Proc. SPIE*. 2002, **4778** pp. 127–130

[23] HAN, S, Novak, E, Wissinger, J, et al. Surface profiler for fixed through glass measurement. *Proc. SPIE*. 2005, **5716** pp. 189–197

[24] DECK. LL. High precision interferometer for measuring mid-spatial frequency departure in free form optics. Optifab 2007: Technical Digest. *SPIE Technical Digest*. 2007, **TD04** p. TD040M

[25] BAUER. W. Special Properties of Coherence Scanning Interferometers for large Measurement Volumes. *J. Phys. Conf. Ser.* 2011, **311** p. 012030

[26] SHEPPARD. CJR and Larkin, KG. Effect of numerical aperture on interference fringe spacing. *Appl. Opt.* 1995, **34** (22) pp. 4731–4733

[27] DE GROOT. P and COLONNA de LEGA, X. Signal modeling for low coherence height-scanning interference microscopy. *Appl. Opt.* 2004, **43** (25) p. 4821

[28] DE GROOT. P. Coherence scanning interferometry. In: *Optical Measurement of Surface Topography*, (LEACH R.ed.). Springer Verlag, Berlin, First Edition, 2011, pp. 187–208.

[29] HANEISHI. H. Signal processing for film thickness measurements by white light interferometry. *Graduate thesis, Department of Communications and Systems Engineering, University of Electro-communications, Chofu, Tokyo*, 1984.

[30] SCHMIT. J. High-speed measurements using optical profiler. *Proc. SPIE*. 2003, **5144** pp. 46–56

[31] SANDOZ. P. Wavelet transform as a processing tool in white-light interferometry. *Opt. Lett.* 1997, **22** (14) pp. 1065–1067

[32] DE GROOT, P and DECK, L. Surface profiling by analysis of white-light interferograms in the spatial frequency domain. *J. Mod. Opt.* 1995, **42** (2) pp. 389–401

[33] RHEE. H-G, Vorburger, TV, Lee, JW and Fu J. Discrepancies between roughness measurements obtained with phase-shifting and white-light interferometry. *Appl. Opt.* 2005, **44** (28) pp. 5919–5927

[34] HARASAKI. A and Wyant, JC. Fringe modulation skewing effect in white-light vertical scanning interferometry. *Appl. Opt.* 2000, **39** (13) pp. 2101–2106

[35] DE GROOT. P, Colonna de Lega, X, Kramer, J and Turzhitsky, M. Determination of fringe order in white light interference microscopy. *Appl. Opt.* 2002, **41** (22) pp. 4571–4578

[36] VDI/VDE 2655, Optical measurement and micro-topographies — Calibration of interference microscopes and depth measurement standards for roughness measurement

[37] SCHMIT. J, Krell, M and Novak E. Calibration of high-speed optical profiler. *Proc. SPIE*. 2003, **5180** pp. 355–364

[38] SCHMIT. J, Olszak, G and McDermed, S. White light interferometry with reference signal. *Proc. SPIE*. 2003, **5180** pp. 355–364

[39] DUBOIS. A. Effects of phase change on reflection in phase-measuring interference microscopy. *Appl. Opt.* 2004, **43** (7) pp. 1503–1507

[40] BOSSEBOEUF. A and Petigrand, S. Application of microscopic interferometry techniques in the MEMS field. *Proc. SPIE*. 2003, **5145** pp. 1–16

[41] DE GROOT. P and Colonna de Lega, X. Interpreting interferometric height measurements using the instrument transfer function. In: *Proc. FRINGE 2005*, (Osten W., ed.). Springer Verlag, Berlin, 2006, pp. 30-37

[42] CHU. J, Wang, Q, Lehan, JP, Gao, G and Griesmann, U. Spatially resolved height response of phase-shifting interferometers measured using a patterned mirror with varying spatial frequency. *Opt. Eng.* 2010, **49** (9) p. 095601

[43] SMITH. WJ. *Modern Optical Engineering*. McGraw-Hill, New York, 1966, pp. 139.

[44] STEWART. JE.. *Optical Principles and Technology for Engineers*. CRC Press, Boca Raton, 1996, pp. 19.

[45] PETZING. J,Coupland, J and Leach, R.. *The Measurement of Rough Surface Topography using Coherence Scanning Interferometry, NPL Good Practice Guide No. 116*. National Physical Laboratory, Teddington, 2011

[46] TAKACS. P, Li, M, Furenlid, K and Church, E. A Step-Height Standard for Surface Profiler Calibration. *Proc. SPIE*. 1993, **1995** pp. 65–74

[47] ISO 4287:1997, *Geometrical Product Specifications (GPS) — Surface texture: Profile method — Terms, definitions and surface texture parameters*

[48] ISO 8015, *Geometrical product specifications (GPS) — Fundamentals — Concepts, principles and rules*

[49] ISO 10934-2:2007, *Optics and optical instruments — Vocabulary for microscopy — Part 2: Advanced techniques in light microscopy*

[50] ISO 14253-1, *Geometrical product specifications (GPS) — Inspection by measurement of workpieces and measuring equipment — Part 1: Decision rules for proving conformity or nonconformity with specifications*

[51] ISO/TR 14638, *Geometrical product specification (GPS) — Masterplan*

[52] ISO 14978:2006, *Geometrical product specifications (GPS) — General concepts and requirements for GPS measuring equipment*

[53] ISO 25178-2:2012, *Geometrical product specifications (GPS) — Surface texture: Areal — Part 2: Terms, definitions and surface texture parameters*

[54] ISO 25178-3:2012, *Geometrical product specifications (GPS) — Surface texture: Areal — Part 3: Specification operators*

[55] ISO 25178-6:2010, *Geometrical product specifications (GPS) — Surface texture: Areal — Part 6: Classification of methods for measuring surface texture*

[56] ISO 25178-601:2010, *Geometrical product specifications (GPS) — Surface texture: Areal — Part 601: Nominal characteristics of contact (stylus) instruments*

[57] ISO 25178-602:2010, *Geometrical product specifications (GPS) — Surface texture: Areal — Part 602: Nominal characteristics of non-contact (confocal chromatic probe) instruments*

[58] ISO 3274:1996, *Geometrical Product Specifications (GPS) — Surface texture: Profile method — Nominal characteristics of contact (stylus) instruments*

[59] ISO 9334:2012, *Optics and photonics — Optical transfer function — Definitions and mathematical relationships*

ICS 17.040.20

Price based on 41 pages